Many thanks to the reviewer for his/her valuable comments and suggestions, which we have addressed as follows (the reviewer's comments are in italics, our reply is in blue standard text):

Anonymous Referee #2
Received and published: 22 July 2015

Major comments

The paper describes data from the SID-3 and PPD, both of which are new instruments designed for mixed-phase and ice cloud studies. The paper is well written and includes a wide range of observations.

However, I have two major issues with this paper. The key weakness of the SID class of instruments is the extended sample volume of the main detector which, for typical mixed-phase clouds, leads to a high probability of two particles in the sample volume. This will lead to a false identification of small ice. The authors for the most part ignore this and concentrate on the coincidence of two particles within the much smaller trigger volume. The identification of a small number of just nucleated ice within a large population of drops is the key measurement requirement of mixed-phase clouds. Only at the end of the paper do the authors discuss this problem and a manual classification of the scattering pattern images. Only with this manual reclassification is it possible to use SID-3 in mixed-phase cloud and there are no details on how this reclassification is done. The second issue is the discussion of ice crystal habit classification using the FFT of the scattering pattern. Again there are no details of how well this works, just that it does. For example what is particle size range, or the effect of particle orientation. Is it really only capable of distinguishing between irregular crystals and 'other habits'?

The referee raised two major concerns (1. Coincident particle sampling; 2. Crystal habit classification) which will be addressed in the following.

1. Coincident particle sampling by the SID-3 main detector (camera). We agree with the referee, however this issue is different for the SID-3 and the PPD-2K. In the case of the PPD-2K the sample flow is focused on the laser beam. Thus we do not expect an extended sensitive volume of the PPD-2K camera and assume the considerations performed for the PPD-2K to be correct.
   In order to investigate coincident particle sampling by the SID-3 camera, we determined the FOV of the SID-3 as follows. We applied a forced trigger signal onto the camera and placed a particle on a nonreflecting glass slide. The glass slide was mounted on a x-y-z stage and moved in the SID-3 laser beam. The procedure is added to the manuscript (page 5 line 13-16) and will be the subject of a publication which is currently in preparation (Schnaiter et al.). From these measurements we derived a sensitive area of the camera of 9mm^2. Using eq. 1c) we calculated the probability for coincident sampling as 0.04% to 7.03% for particle number concentrations of 20 to 300 cm^{-3}. A coincident sampling probability of 7% is significant however scattering patterns from coincident particle sampling by the SID-3 camera were removed as part of the manual inspection of the patterns. We added the description on how to determine the

FOV (page 5 line 13-16) of the SID-3 camera to Sec. 2.1. and added a new subsection 2.3.1 on coincident particle sampling by the SID-3 camera. Furthermore we investigated this issue within the presented field measurements. In the presented section of the VERDI flight 7 ($n \sim 100 cm^{-3}$) 0.21% of the SID-3 scattering patterns showed artifacts. The artifacts can be caused by coincident particle sampling as well as e.g. sampling of a particle at the edge of the sensitive volume. Thus this example illustrates that the given theoretical values should be regarded as an upper boundary for coincident particle sampling by the SID-3 camera and is included in the new manuscript page 23 line 3-8.
For the manual reclassification: The core purpose of the manual reclassification is to classify droplets with artifacts (displayed in the right panel of Fig. 15) as droplets. This step is needed because the v_{az} values of such patterns are increased by the artifacts and they are classified as ice by the algorithm. Thus the reclassification focuses on particles in the vicinity of the shape discrimination threshold v_{az}^{thr} like mentioned on page 22 line 4. With regards to the example images with artifacts we added a statement on page 21 line 26-29.

2. The second issue put forward by the referee is about the habit classification carried out in this work.
This consideration is based on the work of Ulanowski et al. 2006. Let us regard for example the scattering pattern of a columnar ice particle in Fig. 1 c). The corresponding particle is a column which is aligned top to bottom in 9 to 3 o'clock (as seen from the camera) perpendicular to the incident beam direction. By a rotation in the plane perpendicular to the incident beam direction e.g. by 90° to the position 12 to 6 o'clock the scattering pattern will be rotated by 90°. The presented habit classification is based on the Fourier transformation of the azimuthal profiles (Fig. 2). Thus such a variation in particle orientation in the would lead to a shift of the profile along the x- direction only. The Fourier transform and thus the classification is unaffected by such a shift.
However, if the particle of Fig. 1 c) rotates to be parallel to the incident beam direction, the pattern will be affected differently. In the case that the particles basal facet (top or bottom) faces the camera, the particle appears to have six fold symmetry as seen by the camera. Thus a scattering pattern like in Fig. 1. d) will be generated. For intermediate orientations the scattering pattern of the hexagonal column will be a mixture of Fig. 1. c) and d) with bended arcs (see Ulanowski et al. 2006 (Fig 12)). This ambiguity in the detection of columnar and plate like particles with six fold symmetry is the reason why we combine the classes of columnar and hexagonal particles into a single pristine particle class. We added this paragraph to Sec. 2.3.3 (page 12 line 7-25).
The size of the particle determines the size of the speckles in the scattering images (Fig.1). This determines the angular extend and height of e.g. maxima in the azimuthal profiles (Fig2.). However, we expect the Fourier transform of the azimuthal profile, which is used for the shape determination (Supplementary Fig. 3), to be very robust against such variations. Thus the dependence of the shape classification on size is expected to be weak in the size range under investigation (~3-100µm).

Minor comments

Abstract, line 11: There is no evidence within this paper for ice crystal habit classification, and roughness is not defined nor reported in any detail.

We introduce the shape classification in (Sec. 2.3.4) and utilize this information for Fig. 14. Furthermore, quantitative ice shape information from AIDA and VERDI data has been added in the revised manuscript on page 20 line 5-6 (AIDA) and page 23 line 1-2 (VERDI).
The section on ice particle roughness (Sec. 2.3.4 in the old manuscript) was removed and will be subject of a separate publication (Schnaiter et al. 2015). Thus we deleted the word roughness.

Introduction, line 1: The observation of small ice particles indicates recent ice formation by droplet freezing, ice multiplication processes and heterogeneous ice nucleation.

We agree with this statement and would like to direct the reader to page.2 line 25-26.

Introduction, line 7: Other instruments and techniques are mentioned but the ability to phase discriminate is dismissed quickly. Can the authors include the minimum particle size for which these other instruments are able to properly discriminate the phase.

To our best knowledge one cannot discriminate the phase of particles below 20µm with holography or classical optical methods (imaging probes). However among the probes that analyze scattered light there are promising approaches. E.g. utilizing the depolarization signal like in the CPSPD (Baumgardner et al. 2014) allows for a phase discrimination of particles with sizes below 20µm. However this method is dependent on particle orientation. We modified our statement accordingly (page 3 line 10-13).

Introduction, line 15: The scattering pattern observed with both the SID-3 and PPD also depends on the particle orientation. This dependence is not really discussed later in the paper but this weakness is crucial to understanding how well the crystal habit classification works.

We agree with the referee that the scattering patterns depend on orientation. As already outlined above (major comment 2), we added a discussion on the dependence of shape classification on particle orientation. We identified an ambiguity for hexagonal ice and this is the reason why we combine the classes of columnar and hexagonal particles into a single pristine particle class. We therefore modified Sec. 2.3.3.

Methods, SID-3 and PPD, line 24: The authors mention sensitive volume throughout the paper, but do not make it clear what volume they mean. For both the SID-3 and PPD there are two particle detecting volumes, the first defined by the trigger optical detector with simple pulse height and timing, and the second defined by the main optical detector with the detailed scattering pattern. The second main detector volume is much larger

than the trigger volume which leads to high probability of second particles (other than that causing the trigger) to add to the scattering pattern.

We adapted the manuscript in order to clarify the respective sensitive volumes (is equal to (sensitive area) x (depth of the laser beam)).
In the case of the PPD-2K the sample flow is focused on the laser beam. Thus we do not expect an extended sensitive volume of the PPD-2K camera and the sensitive volume of PPD-2K trigger detector and camera should be identical. Thus we think our coincidence considerations for the PPD-2K are correct and apply for both its trigger detector and camera.
In the case of the SID-3 we introduce two sensitive areas in the new manuscript, one for the SID-3 trigger detectors and one for the SID-3 camera (page 5 line 11-17). With regards to the trigger detectors we state that the smaller FOV of trigger one (0.47 mm^2) lies within the larger FOV of trigger two (1.35mm^2). For the coincident particle sampling by the trigger detectors we considered an extended FOV which is the FOV of trigger two. We think this can be taken as an upper bound for coincident particle sampling by the SID-3 trigger detectors.
With regards to the issue of coincident particle sampling by the SID-3 camera we used the corresponding FOV and found coincidence probabilities mentioned in the reply to the major comments and a respective paragraph Sec 2.3.1 was added to the manuscript.

*Methods, SID-3 and PPD, line 17: The authors need to make it clear that 0.47mm2 is the trigger sensitive area (and 0.47*0.16=0.075mm3 the trigger sensitive volume). The sensitive area for SID-3 main detector is defined by the laser width and camera optics, probably around 1.2mm*8mm=9.6mm2 as discussed in Johnson et al 2014.*

We agree with the referee that the SID-3 camera has a different and extended FOV which we determined to be 9mm^2 (page 5 line 11). We determined this area by applying a forced trigger signal to the camera and moving a particle on a nonreflecting glass slide through the SID-3 laser beam. We used this information to add Sec. 2.3.1. to the manuscript.

Methods, SID-3 and PPD, line 20: The sensitive area of the PPD is specified as 2.5mm2. This is a key property of these instruments and the authors should include the justification for using this. Is it for example, defined by the air stream focusing system with the PPD optical cell? If so, what range of sample flow rates is this valid for.

We mentioned in the manuscript that within the PPD-2K the sample flow is focused on the larger laser beam (page 4, line 21). A = 2.5mm^2 is the cross section of the focused sample flow for flow rates in the range of 4-7l/min which we used for the measurements for this work. The respective tests were performed by the University of Hertfordshire. E. Hirst is included in the manuscript as the respective reference (page 8 line 22).

Analysis, coincident particle sampling, line 20: Only coincident sampling for the trigger sensing volume is discussed. This is the main weakness of the paper. The authors

correctly state that coincidences are not an issue for particle concentrations often observed in clouds, but this is true only for the information from the trigger system, particle size derived from the pulse height recorded by the trigger PMT. Coincidences where two particles are within the much larger main detector sensing volume is not mentioned.

We thank the referee for this hint and included a discussion of coincident particle sampling by the SID-3 camera in the major comments and in the manuscript in a new subsection Sec. 2.3.1. Furthermore we used these findings in the discussion of the artifacts observed within the presented CLACE 2013 (page 21 line 27-28) and VERDI (page 23 line 4-8) measurements.

Analysis of scattering patterns, line 25: What is the resolution of the 'grey levels', is it 0 to 255 (8-bit) or higher?

The cameras of the SID-3 and PPD-2K are capable of generating 12 bit images (Ulanowski et al. 2014). However, for this work we used scattering patterns recorded with 8bit pixel depth only. The reason for that is that the image file size increases by a factor of 6.5 from 8 to 12bit. This implies that the acquisition rate of the instrument decreases. In a MPC many and mainly droplet patterns are recorded. For a droplet there is no benefit of an increased pixel depth. Thus the presented data was recorded with 8bit only which however means a potential loss of information for ice particles.

Analysis of scattering patterns, line 1: The criteria for rejection of q<0.2 will bias the sizing and ice crystal habit classification. The authors need to discuss this in more detail.

Applying a criteria of q<0.2 leads to the rejection of patterns which have more than 20% saturated pixels. The camera gain can be adjusted which means that the number of saturated pixels can be adjusted for a given particle population. q>0.2 typically holds for patterns which are out of the size range of interest for our investigation (very large particles) and we do not focus on the number, size, and shape of these particles. Furthermore, our sizing is based on the trigger signals which are not altered by rejecting scattering patterns.
With regards to the shape discrimination it is true that the habit classification is changed by such a criterion from an assigned shape to the shape "rejected". As the q criterion only applies for particles which are larger than the size range in the focus of investigation, findings on a defined size range of particles stay unaffected.
A corresponding statement on the q criterion was added to the manuscript (page 8 line 12).

Analysis of scattering patterns, equation 2: The variance Vaz is different to the asphericity Af used in Cotton et al 2010 and Johnson et al 2014. Is Vaz better than Af in terms of being able to discriminate drops and crystals? What is the value of N and what is the minimum number that still gives discrimination. For example, SID-2 has 28 azimuthal detectors so N=28. This is enough to discriminate drops and ice crystals in

mixed-phase cloud, but it not enough to identify and reject coincident images where two particles are in the detector sensing volume. Knowing the minimum N would be very helpful if SID-2 where to be improved with higher resolution detectors (the CCD technology in SID-3, while high resolution, is slow).

The higher resolved SID-3 patterns provide more information and should thus allow for a better phase discrimination than patterns from earlier SID instruments. Thus v_{az} should be better than A_f for phase discrimination. We added a corresponding statement on page 8 line 25-27.
We agree with the referee that knowing a minimum N would be interesting, but this issue would need detailed side by side lab tests of the SID-2 and SID-3. To our knowledge this was not done so far and is the reason why we think that an answer to that question is beyond the scope of this work.

Size calibration, line 21: What is the accuracy of the drop sizing using the Mie angular dependence and how does this compare with the usual CDP type of measurement? What is the minimum size, presumably it is when the first secondary peak (those at 12 degrees in figure 3) is within the angular coverage of the detector.

The accuracy of the Mie-fit is highly dependent on how well the droplet scattering pattern is centered. The sensitive area of the SID-3 trigger detector (0.47mm^2) is smaller than that of the PPD-2K (2.5mm^2). Thus the error in sizing of the SID-3 is smaller than that of the PPD-2K. We estimate 10% as an upper bound for the error of the sizing by a Mie fit. Our algorithm also performs a fit when the profile is monotonically decreasing. A monotonically decreasing profile corresponds to particles of about 1.5µm, which is what we would assign as the detection threshold of the Mie-fit algorithm. Please note that the size detection threshold of the instruments was 3µm at minimum (see panels c) of Figs. 8, 9, 12, 13, 17).
For a comparison to a CDP type instrument it is important to regard the theoretical data points in Figs 5, 6, 7 (left panels). There are no distinct ambiguities (although fluctuations) in these curves. Thus the sizing bases on the trigger signal/ image intensity of the SID-3 and PPD-2K should be clear on a scale of ~0.5µm. This means an advantage compared to the CDP sizing with ambiguities in the range of µms e.g. as displayed in Fig 4 of Lance et al 2000.
We added a corresponding statement on page 10 line 25-26.

Size calibration, line 8: Is the larger collection angle of the SID-3 trigger the reason for the increased irradiance between figures 4 and 5?

The half angle of the SID-3 trigger detector is +/-9.25° at 50° relative to the forward direction. The PPD-2K trigger detector collects light in 7.4° to 25.6° relative to the forward direction. This causes the difference in the theoretical values. A significant contribution to the spread of the experimental values is electronic noise. This statement is added to the caption of Fig. 5.

Size calibration, line 20: The non-linear behaviour of the camera image intesifier leads to the key conclusion that the main detector signal cannot be used for particle sizing. Can the authors plot the trigger signal versus the main detector signal to show more clearly this non-linearity. They should then change the image selection criteria q<0.2 to see if this is causing the non-linear behaviour.

The size calibration involves droplet patterns only. In the presented dataset no droplet pattern (the maximum droplet size was 25µm) showed q>0.2. Thus the right panels of Figs 4 and 6 do not change by changing the q-criterion. A remark at the introduction of the q-value was included in the manuscript (page 8 line 11-12).
The plot of the mean image intensity vs. the trigger intensity is included below as Fig 1 and illustrates the nonlinear behavior of the mean image intensity against the trigger intensity.

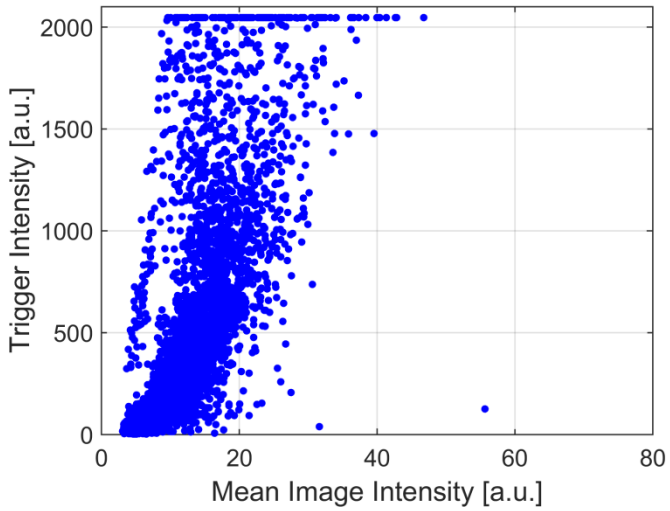

Figure 1: Trigger Intensity against the mean image intensity.

Ice particle shape classification: This is a key capability of the SID-3 and PPD but the authors do not really show how well this works. The scattering pattern depends on particle orientation as well as habit.

It is true that the scattering pattern depends on particle orientation as well as habit. The effect of orientation was discussed above in the major comments and we modified Sec. 2.3.3. The effect of orientation leads to an ambiguity, which is the reason why we combine the classes of columnar and hexagonal particles into a single pristine particles class. Thus a classification of ice particles as irregular or pristine is robust against a variation of the particles orientation. (page 12 line 23)

Roughness analysis: This is mentioned briefly here but no other results or analysis. This section should be removed.

The section (Sec. 2.3.4. in the old manuscript) was removed like suggested by the referee.

Quantification of specific particle types, line 24: The equation for Pthr=0.023 s/Tav, I assume that the s is seconds and should not be in the equation.

The formula was changed to: $Pthr=a/t_{av}$, with a = 0.023s. (page 14 line 17)

AIDA cloud chamber measurements, line 16: What do the typical scattering patterns look like for ice during the RICE 03 expansion, are they columns, plates or irregulars?

During the mixed phase period of AIDA Expansion 46 (100s < t < 500s) the PPD-2K detected 532 ice particle scattering patterns. and 10.1 +/- 1.5% of these patterns were pristine, whereas 89.9 +/- 5.7% were irregular. These numbers illustrate that the vast majority of ice particle scattering patterns detected in MPCs at the AIDA is irregular. This information is included in the manuscript (page 20 line 6-8). For a significant amount of pristine ice particles is generated at the AIDA in pure ice clouds which will be subject of Schnaiter et al.

AIDA cloud chamber measurements, line 27: Why is the size detection threshold of the PPD so much higher than SID-3? Is it related to the angular coverage of the trigger detector? This does not explain the factor of five discrepancy in the total number concentrations in figure 11 between the PPD and the WELAS/SID-3 because according to figure 10, most particles are above the 7micron threshold.

The used PPD-2K shows a rather high level of electronic background noise. This is the reason why the detection threshold had to be raised. We are currently working on a solution to this problem.
Figure 10 is a scatter plot and thus not suited to derive a particle number concentration. The concentration of particles can more easily be derived from fig. 8 c). The lowermost bin of the SID-3 number size distribution shows a significant density and has an upper limit of 7.1µm. This means most of the particles in the lowermost size bin measured by the SID-3 are not detected by the PPD-2K. This explains the discrepancies in Fig. 11. We added a corresponding remark to the manuscript to clarify this (page 19 line 8-9).

Measurements during CLACE, line 14: In figure 15 the overlap between drops and ice crystals is explained as coincidences where two particles are in the sensing volume of the main detector. This coincidence is the big weakness of the SID class of instruments in mixed-phase cloud where the many small drops lead to a false signal of ice. The authors manually identify 2460 images out of 133,284 where coincidence of drops give a high Vaz (1.8%). Figure 11 indicates that the drop concentration was below 20cm-3, and using equation 1, the sensing volume of the main detector can be calculated as 9.5mm3 (as discussed in Johnson et al 2014).

In this context we would like to mention that by looking at the scattering patterns with artifacts in the right panel of fig. 15, one intuitively assumes that the black regions of the scattering patterns display the shadows of a second particle in the light path. However,

one needs to keep in mind that the scattering pattern is obtained in the Fourier plane. We succeeded to generate scattering patterns with similar artifacts in the laboratory when injecting single droplets at the edge of the sensitive volume. For these tests, we used the aforementioned piezoelectric droplet generator, which ejects only one droplet at time.

While sampling clouds with a high density, the probability of imaging a particle at the edge of the sensitive volume might be increased by a second particle being present in the vicinity of the sensitive area.
The scattering patterns with artifacts displayed in Fig. 15 were recorded during CLACE 2013 which took place on the Jungfraujoch and are displayed in Fig. 13. Fig. 11 shows measurements from the AIDA cloud chamber, where no scattering patterns with artifacts were observed.
During the field measurements during CLACE 2013 and during VERDI we observed scattering pattern with artifacts. These artifacts should be caused by coincident particle sampling as well as sampling at the edge of the sensitive volume. This is discussed on page 21-22 line 26-2 CLACE and page 23 line 4-9 VERDI.

Conclusion, line 3: The crystal shape deduction has not been adequately discussed and the roughness should not be mentioned.

We removed the roughness and adopted Sec. 2.3.3 Ice particle shape classification. In addition we included shape deduction from AIDA and VERDI measurements. Furthermore, a plot of further sample particles illustrating the shape classification and of the Fourier coefficients from the analysis of the scattering patterns of Fig. 1 was added to the supplementary material (Supplementary Fig. 3).
We are aware that the shape deduction can be expanded but we only distinguish irregular from pristine ice particles. The argument for this is the ambiguity in classifying an hexagonal ice particle like outline in the replies to the major concerns.

Conclusion, line 8: The comparison of the total number concentrations, in figure 11, shows significant disagreement.

We agree that there is a discrepancy in the number concentrations. However, this can be understood by comparing the number size distributions from figs. 8 c) and fig 9 c) (see comments above). A remark was added to the manuscript to clarify this point (page 19 line 9).

Figure 1: What is the gamma correction?

The gamma correction is used to increase the brightness of the displayed images. It is only a display setting and an easy description can be found e.g. under http://www.graphics.cornell.edu/~westin/gamma/gamma.html.

Figure 2: Why is the droplet azimuthal distribution not exactly flat? Is this scattering pattern not exactly central?

It is correct that the droplet scattering pattern is slightly skewed. The PPD-2K is more prone to this as its sensitive area is 2.5mm^2 compared to 0.47mm^2 of the SID-3.

Figure 5: Is the band of scattered points to the right of the main band from coincidences? Can the authors include some scattering images.

The data points displayed in fig. 5 are successfully fitted droplet patterns only. These patterns show a very low azimuthal variance, no artifacts and are almost perfect Airy discs. We therefore decided not to include further images but the corresponding patterns are similar to Fig. 1a). The spread of the intensities is caused by noise in the trigger signal and electronics. A statement is added to the caption of the Fig. 5.

Figure 7: If a future camera had higher sampling rate, how would the lines move?

A higher sampling rate of the camera would lead to more information and thus the ice detection threshold would decrease (move down).

Figure 15: This if similar to the scatter plots in Cotton et al 2010. Can the authors plot cumulative PDFs as in figure 9 of Cotton et al 2010 for comparison.

A corresponding figure is included as supplementary Fig. 2. The overlap in the v_{az} values of the scattering patterns classified as droplets and as ice particles is clearly visible and indicates the need for a manual reclassification.